Proceedings of the International Symposium on Engineering Lessons Learned from
the 2011 Great East Japan Earthquake, March 1-4, 2012, Tokyo, Japan

Mechanism of Slope Failures in Residential Land on Fill during Great East Japan Earthquake

Masayuki Hyodo[1], Rolando Orense[2], Shohei Noda[3], Satoshi Furukawa[4], Toshihiko Furui[5]

[1] Professor, Department of Civil Engineering, Yamaguchi University,
Yamaguchi, Japan, hyodo@yamaguchi-u.ac.jp
[2] Professor, Department of Civil Engineering, University of Auckland,
Auckland, New Zealand, r.orense@auckland.ac.nz
[3] Student, Department of Civil Engineering, Yamaguchi University,
Yamaguchi, Japan, r003wf@yamaguchi-u.ac.jp
[4] Frontier Project Section, Chuden Engineering Consultants Co. Ltd.,
Hiroshima, Japan, furukawa@cecnet.co.jp
[5] Etajima City Office, Hiroshima Prefecture,
Hiroshima, Japan, furui@mbf.ocn.ne.jp

ABSTRACT: As a result of the Great East Japan Earthquake, five slope failures occurred in a residential area on artificial valley fills in Taiyo New Town, Yamamoto, Miyagi Prefecture. The fill material is sandy, derived from the weathering of tuffaceous sandstone which formed the natural ground. Cyclic triaxial tests showed that the fill, which has about F_c=20%, has very low liquefaction resistance, which decreased with application of initial shear stress. Thus, the slope failure in Taiyo New Town can be attributed to the liquefaction of the fill material induced by the intense shaking.

Key Words: Great East Japan earthquake, slope failure, valley fill, pseudostatic analysis, tuffaceous sandstone, liquefaction

INTRODUCTION

With moment magnitude M_w 9.0, the gigantic 2011 off the Pacific coast of Tohoku Earthquake caused extensive damage to life and property in Tohoku and Kanto regions in eastern part of Japan. One of the worst hit areas is the coastal town of Yamamoto on southern part of Miyagi Prefecture. Almost 24 km^2 of the town's 64 km^2 area, or about 38%, was flooded and destroyed by the large-scale tsunami generated by the earthquake (GSI, 2011). Most of the inundated area was on the eastern side of the National Route 6. In addition, several slope failures occurred on the hilly areas located to the west of Route 6. In terms of slope failures, one of the worst-hit areas was Taiyo New Town, a housing site located on artificial valley fill just to the west of Route 6. The site was constructed by leveling the hilly area and using the cut materials as fills for the valleys to provide viable land for residential purposes. Following the earthquake, slope failures occurred in five different sections of the land,

damaging houses, roads, park and pipelines. In one of the failed sites, the debris slid and covered a parking lot just on the side of Route 6.

Following the earthquake, site investigations were performed at the site in order to clarify the causes(s) of the slope failures. Samples were obtained at several locations adjacent to the failed slopes and laboratory tests were conducted to investigate their geotechnical properties. Finally, slope stability analyses were conducted in order to better understand the response of the embankment to earthquake loading. The results highlighted the seismic vulnerability of residential areas on artificial valley fills like Taiyo New Town that are constructed with weak tuffaceous materials as fill.

DESCRIPTION OF THE AREA

The Taiyo New Town housing site is located in the central part of Yamamoto, a coastal town on the southern edge of Miyagi Prefecture. It is located on the hilly region to the west of Route No. 6, which traverses the prefecture in almost northwest-southeast direction. In fact, Route 6 appears to be the dividing line between the coastal plain on the east and the 40-50m high mountains (Wariyama uplift zone) on the west of the prefecture.

The site of the residential area was developed in the 1970s by cutting and leveling off some parts of the hills and using the materials as fill for the valleys. Figure 1 shows the depth distribution of cuts and fills in Taiyo New Town. To level off the residential land, cuts were made on the hills as high as 8-10m, while valley floors as deep as 10-15 m were filled up using the same materials that were cut from the elevated regions. It can be observed that deep valleys existed in the central portion and in western boundary of the site. The eastern side of the site adjacent to Route 6 was also filled up, with embankment having slope of 1:1.5. The elevation of the filled-up residential site was about 35 m above mean sea level. It has an area of about 0.12 km^2 and when the earthquake struck, more than 200 houses have been built at the site.

Investigation of the local geology of the site revealed that the original ground consisted of tuffaceous sandstones of the Yamamoto Formation. Subsequent boring data showed that the sandstones were weakly consolidated and exhibited high degree of weathering towards the surface, with the surficial layer appearing like sandy soil. Thus, the material used to fill up the valleys consisted of sandy soils from the weathered tuffaceous sandstones. Standard penetration tests indicated that the sandy material used as fill has an average *N*-value of 5, while the highly weathered top layer and the weathered layer the sandstone has average *N*-values of 6 and 16, respectively.

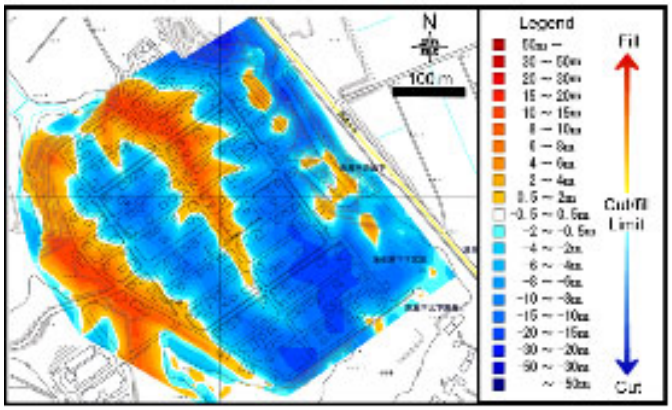

Figure 1. The housing site foundation map of Taiyo New Town, showing the thickness distribution of cut and fill sections (Fukken Gijutsu Consultant, 2008)

STRONG MOTION STATION AND SEISMIC RECORDS

About 2km to the south of Taiyo New Town, the National Research Institute for Earth Science and Disaster Prevention (NIED) operates a KiK-Net seismic station (MYGH10: Yamamoto Station) with digital strong-motion seismometers installed at the ground surface and at a depth of GL-205m. The 2011 Tohoku earthquake triggered many seismic stations in the area, including the one in Yamamoto, and recorded strong motions. Figure 2 shows the acceleration time histories recorded at the station, both on the surface and at depth, while Figure 3 illustrates the corresponding Fourier spectra of the acceleration records. The peak accelerations recorded at depth were in the range of 150~220 cm/sec^2 with predominant frequency of 0.35 Hz. On the ground surface, on the other hand, the peak values were much higher, 850~870 cm/sec^2, with the predominant frequency shifting to 4-6 Hz.

The soil profile at KiK-Net Yamamoto station is shown in Table 1. It can be observed that tuffaceous sandstone with shear wave velocity V_s<770 m/sec exists in the vicinity of the seismometer installed at the bottom of the borehole. Moreover, the upper layer generally consisted of pumiceous tuff and tuffaceous sandstones. This profile generally amplified the seismic motion as it propagates towards the ground surface.

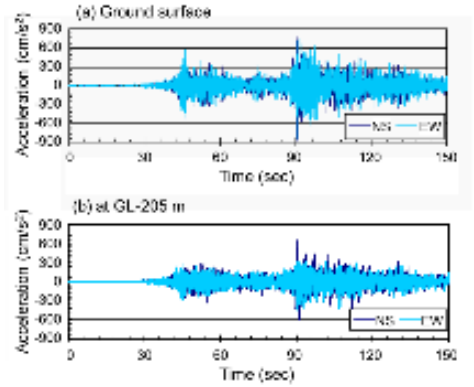

Figure 2. Acceleration time histories obtained from Yamamoto KiKNet Seismic station: (a) at ground surface; (b) at GL-205m (data from KiK-Net website)

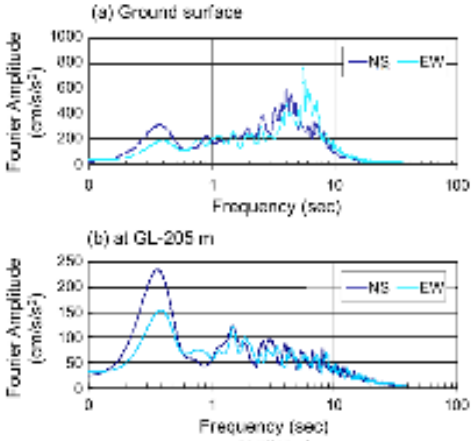

Figure 3. Fourier spectra of acceleration records obtained from Yamamoto KiKNet Seismic station: (a) at ground surface; (b) at GL-205m

Table 1. Soil profile at Yamamoto Kik-Net seismic station (MYGH10) (data from Kik-Net website)

Depth (m)	Thickness (m)	Type of soil/rock	V_p m/s)	V_s (m/s)
2.0	2.0	Clay	500	110
3.5	1.5	Clay	1750	250
8.0	4.5	Sandstone	1750	390
18.0	10.0	Conglomerate	1750	390
34.0	16.0	Sandstone	1750	390
42.0	8.0	Pumiceous tuff	1830	590
114.0	72.0	Tuffaceous Sandstone	1830	590
142.0	28.0	Sandstone	1920	770
178.0	56.0	Tuffaceous sandstone	1920	770
208.0	30.0	Silt	1920	770

OUTLINE OF DAMAGE

Following the 2011 earthquake, slope failures occurred at five sites within the Taiyo New Town housing site. The locations of the slope failure are shown in Figure 4. These failed or slid blocks were sequentially numbered, starting with Failed Block 1 on the eastern boundary of the housing site, going counterclockwise to Failed Block 5 on the western side. Block 1 consisted of two landslides, referred to as Block 1-1 and Block 1-2, respectively. Also shown in the figure are the locations of damaged roads due to the slope failure and damaged road pavements. Extensometers were placed on the eastern boundary to monitor the movement of the fill. In addition, several standard penetrations tests were performed within the fill and adjacent to the failed blocks.

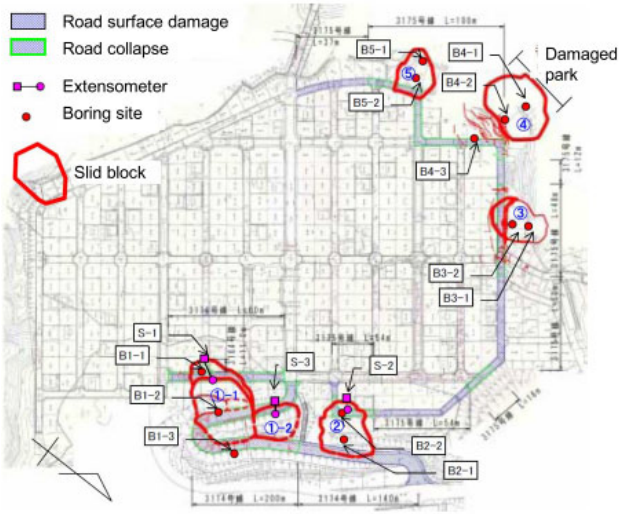

Figure 4. Location of failed slopes in Taiyo New Town

Comparing the locations of the failed blocks in the housing site (Figure 4) with the foundation ground map shown in Figure 1, it is clear that all failed slopes occurred either on the edge of the valley fill or on the shoulder of the embankment. This suggests that the fill material, rather than the natural ground, was involved in the slope failures.

Failed Block 1

Block 1 consisted of two slope failures. The first sliding block, 1-1, caused settlement at the crest and laterally flowed down the sloping ground, as shown schematically in Figure 5. As a result, a house located on the laterally moving ground tilted and a 1m high vertical offset was also created. Extensional cracks were also observed on the ground and road pavements. The adjacent failed block, 1-2, was smaller in scope and induced cracking on the road as the sliding mass slid. In both cases, the surface of the road downslope was pushed up.

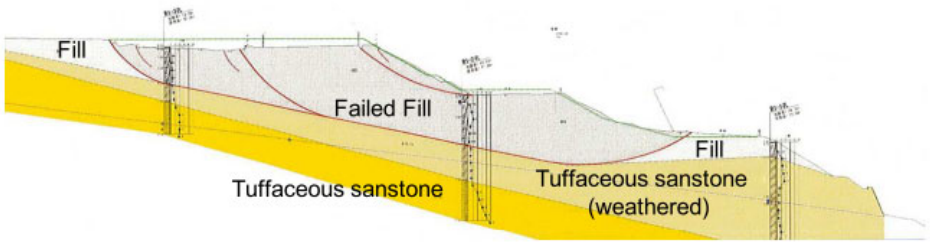

Figure 5. Cross-sectional profile of failed slope in Block 1-1

Failed Block 2

About 50m north of failed Block 1, the shoulder of the embankment collapsed, sending debris 15 m below towards the parking lot adjacent to a convenience store. It is apparent that the failure was confined to the upper layer consisting of fill material. A house located at the crest of the sliding mass was partially destroyed, while the roads positioned at the top and midway of the slope were totally destroyed, sending cracked pavements downward. Just to the north of the failed slope and down on the main road, a reinforced retaining wall missed the landslide. This retaining wall was constructed in 2008 when the section failed following a heavy rainfall; the retaining wall was not damaged by this earthquake.

SOIL AND SITE CHARACTERISTICS

To understand the characteristics of the fill material, soil samples were obtained adjacent to the failed blocks and geotechnical tests were performed.

Geotechnical properties

Soils samples were obtained near failed Blocks 1, 2, 3 and 5 in order to investigate the geotechnical properties of the soil used as fill. Figure 6 shows the grain size distribution curves for samples from the four sites. It can be seen that the curves were fairly similar at all three locations, indicating that the fill materials were uniform throughout the housing site The soil have fairly uniform distribution with fines content, F_c=20%.

Samples obtained from Block 1 site were quite abundant and these were used in most of the geotechnical tests. Index property tests, based on Japanese Geotechnical Society standards (JGS, 2001) showed that the density of the particles was 2.478 g/cm^3, while the maximum and minimum densities were 1.319 and 1.079 g/cm^3, respectively. The compaction curve is shown in Figure 8 where it is seen that the optimum water content is w_{opt}=13.8% corresponding to maximum dry density, ρ_{dmax}=1.822 g/cm^3.

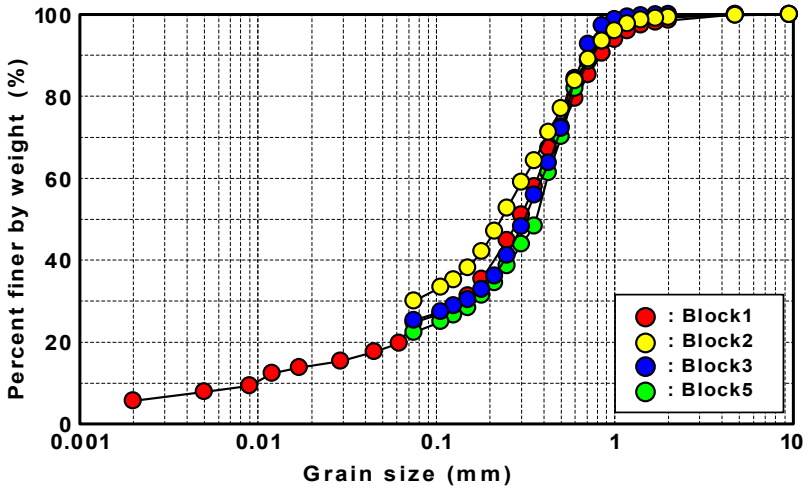

Figure 6. Grain size distribution curves of samples obtained from four sites

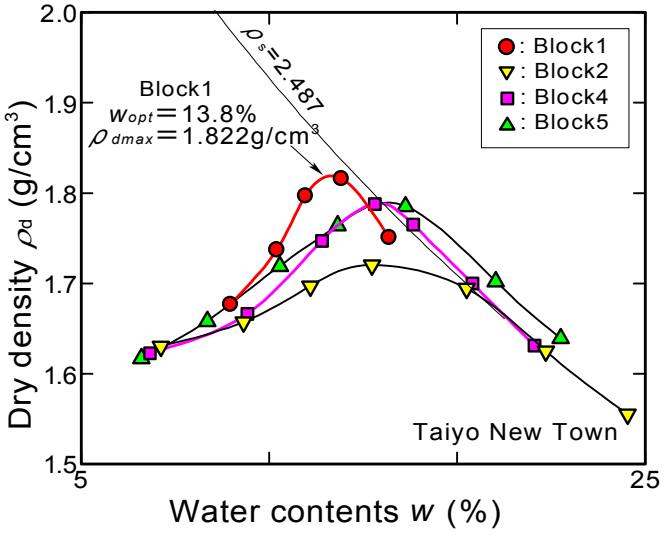

Figure 7. Compaction curve

Next, monotonic drained and cyclic undrained triaxial tests were conducted on the soil samples. In these tests, the reconstituted samples were prepared such that they have dry density equal to 90% of the maximum dry density, i.e., degree of compaction D_c=90%. Using the obtained maximum and minimum dry densities, this corresponds to a relative density D_r=188%. The results of the monotonic drained tests for confining pressure of σ_c'=50, 100 and 150 kPa are shown in Figure 8. The undrained shear test was also performed for confining pressure of σ_c'=100kPa and presented in the figure. The soil shows contractive behavior at all levels of applied pressure. This may be due to the collapsible behavior of weathered tuffaceous sandstone. From the stress-strain relations, Mohr circles of stress were drawn at residual state as shown in Figure 10, and the strength parameters were obtained. The results indicate the following values: cohesion, c=9 kPa, and angle of internal friction ϕ=31.7°. Such internal friction angle is quite low for sandy soils.

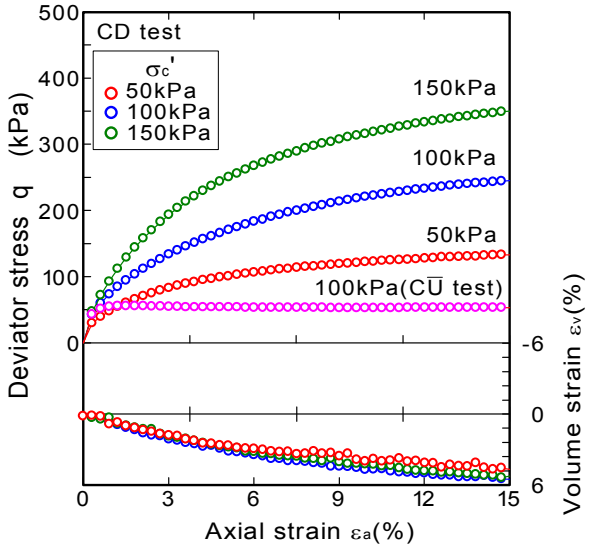

Figure 8. Results of consolidated drained triaxial tests

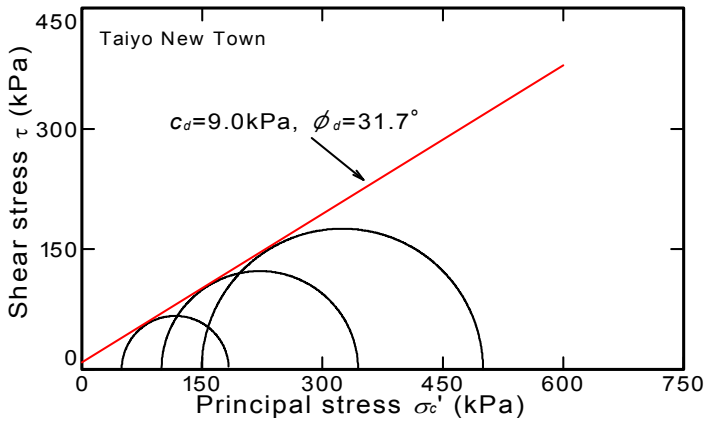

Figure 9. Mohr's stress circles and failure envelope from results by drained triaxial tests

Cyclic undrained triaxial tests were performed on reconstituted samples under isotropically consolidated condition, and the liquefaction resistance curve obtained for a double amplitude axial strain ε_{DA}=5% is shown by the solid circles in Figure 10. It is seen that the liquefaction resistance of the material is quite low, indicating the susceptibility of the material to large deformation when shaken under saturated condition. This may be due to the high fines content of the soil and the density used to prepare the reconstituted specimen. Note that for soil specimens with *Dc*=90%, the dry density of the soil was taken as 1.64 g/cm^3. According to Yamamoto Town Office, dry densities ranging from 1.44-1.54 g/cm^3 were obtained at the site based on previous site investigations. Thus, although the density of the specimen used in the test was higher than the in-situ values, the liquefaction resistance of the soil was low. Although the location of the water table during the earthquake was not confirmed, this type of material will liquefy easily when subjected to cyclic shearing induced by earthquake, and will fail due to reduction in effective stress.

In order to simulate the presence of initial shear stress in sloping grounds, such as in the present embankment, cyclic undrained triaxial tests were also performed on anisotropically consolidated specimens. Results for cases with initial shear stress ratio, $\sigma_s/2\sigma_c$'=0.30, and 0.375 are also indicated in Figure 10. In case of anisotropically consolidated samples, the cyclic failure was defined in terms of peak axial strain ε_p=5%. It appears that if the fill material is subjected to initial static stress, the cyclic strength decreases; such behavior is quite different from those observed for other types of granular

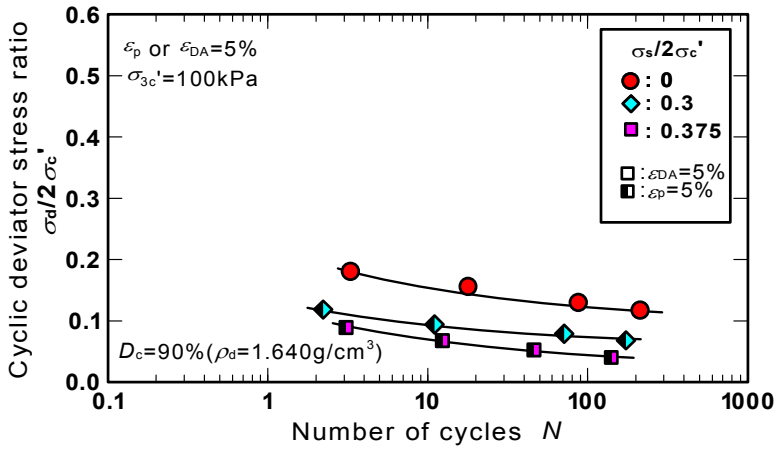

Figure 10. Liquefaction resistance curves of isotropically and anisotropically consolidated samples

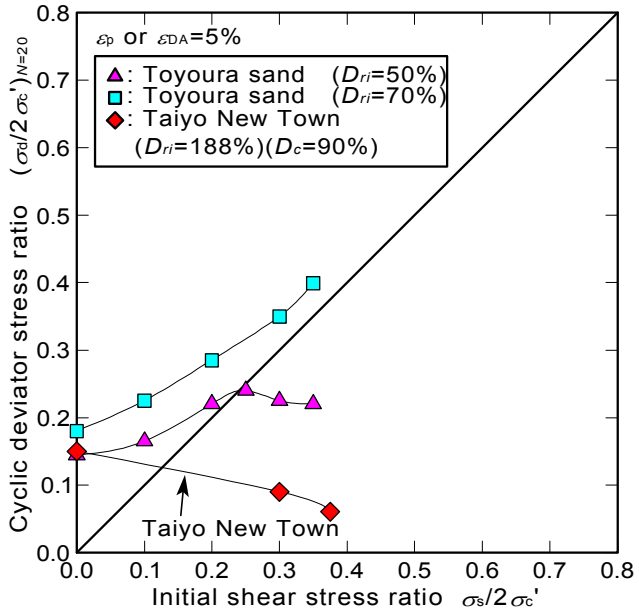

Figure 11. Variation of cyclic strength at N=20 cycles with initial shear stress ratio

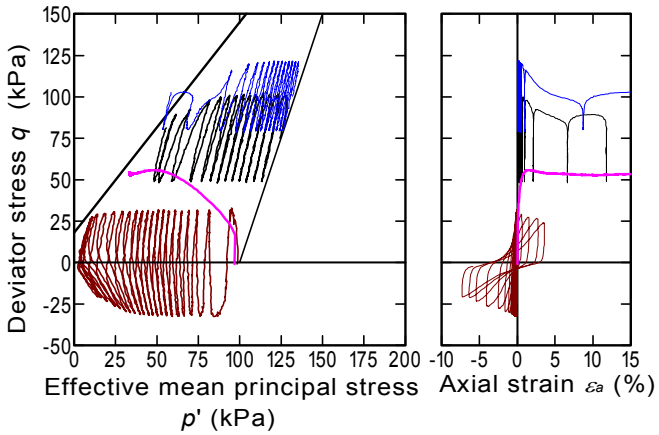

Figure 12. Cyclic stress paths and cyclic stress strain curves for isotropically and anisotropically consolidated samples

materials (Vaid, 1983; Hyodo et al., 1991, 1994; Hosono and Yoshimine, 2004). This confirms that the fill material is indeed weak and susceptible to large deformation under earthquake loading. Figure 11 shows the cyclic deviator stress ratio to cause failure after 20 cycles. The results for Toyoura sand with D_r=50% and D_r=70% are also shown in the figure for comparison. In the case of Toyoura sand, the cyclic strength increases with initial shear stress ratio as expected for medium to dense material. However, in the case of the sampled soil, the cyclic strength decreased with increasing initial shear stress ratio, although it should noted that the definition of failure changed from ε_{DA}=5% to ε_p=5%. Further it should be noted that failure occurred for stress non-reversal condition at the material while stress reversal was necessary to cause failure at dense Toyoura sand.

Figure 12 shows the stress paths and corresponding relationship between cyclic deviator stress and axial strain for both isotropically and anisotropically consolidated samples. Examination of the cyclic stress paths for isotropically consolidated sample shows liquefaction occurring as the stress path cycles through zero effective confining pressure. The development of cyclic strains occurs in both compression and extension. The cyclic failure was defined as a strain double amplitude of 5% (ε_{DA}=5%). On the other hand, the cyclic stress paths for anisotropically consolidated samples shows cyclic failure occurring as the stress path reaches to the failure envelope developed by monotonic shear tests. The corresponding cyclic stress strain plots are shown taken to peak axial strain of approximately 15%. It should be noted that cyclic strain amplitude becomes larger as the stress path approaches to failure envelope. The cyclic strength for anisotropic samples was defined as the number of cycles to reach peak axial strain ε_p=5%.

SLOPE STABILITY ANALYSES

To explain the cause of failure, preliminary analyses were conducted considering the stability of the embankments during the 2011 earthquake under different scenarios. For this purpose, pseudostatic analyses were performed. The equivalent strong motion at the top of the embankment was determined through the procedure outlined in Figure 13. Firstly, the model for the 1-D soil profile at the location of the KiK-net seismic station (Table 1) was verified using earthquake recordings obtained during previous smaller earthquakes of 1 September 2010 and 10 February 2011. In both cases, the time history of acceleration recorded on the ground surface was used as input and the acceleration at the bottom of the borehole (GL-205m) was simulated using the program SHAKE. Next, to incorporate the non-linear response of the soil due to the larger amplitude of motion resulting from the 2011 Tohoku earthquake event, the surface motion (Figure 2a) was used as input to simulate the motion at GL-205m (Figure 2b). Due to space limitation, the details of the calculations are not presented here. Suffice it to say that the 1-D ground model at the seismic station site was sufficiently validated. From the last analysis, the incident wave (2E) at the engineering bedrock, Point C, was calculated for both N-S and E-W direction.

For the purpose of analysis, the cross-sectional profile for Block 1 shown in Figure 5 was used. Using the boring data obtained from field tests and knowing that the natural period of the site is 0.7 sec, the soil profile and corresponding parameters were established, as summarized in Table 2. The depth of the engineering bedrock from the surface of the fill was 34m.

Next, the strong motion obtained at Point C was used as input (2E) at Point B to determine the surface acceleration at Point A. Since Point C and Point B are just 2km apart, attenuation of motion was not considered. Again, seismic response analyses were conducted and the results obtained showed PGAs at point A of 1322.6 and 1171.3 cm/sec^2 in N-S and E-W directions, respectively. Using the equation for lateral seismic coefficient, k_h, proposed by Noda et al. (1975), the obtained PGAs correspond to k_h=0.368 and 0.354, respectively.

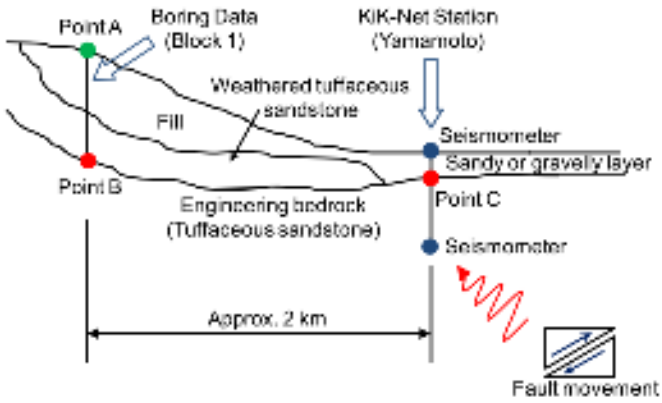

Figure 13. Schematic diagram showing how the PGA on top of the fill was calculated from KiK-Net recorded motions

Table 2. Soil profile and soil properties for failed Block 1 site used in the analysis

Soil Type	Depth (m)	H (m)	SPT N-value	γ_t (kN/m^3)	γ_{sat} (kN/m^3)	V_s (m/sec)	$4H/V_s$ (sec)
Fill (sandy type)	6	6	4.7	17.5	18.9	128	0.19
Tuffaceous sand stone (strongly weathered)	12	6	6.7	18.6	20.6	149	0.16
Tuffaceous sandstone (weathered	34	22	32.4	18.6	20.6	252	0.35
							0.70

In the pseudostatic analysis of slope stability, three cases of ground models and slip failures were considered: Case A, where ground water table is low (effect not considered) with composite slip surfaces; Case B – 1, where ground water table is near the boundary between fill and sandstone with composite slip surfaces; and Case B – 2 where ground water table is near the boundary between fill and sandstone with cylindrical slip surface. In the analyses, the strength parameters obtained from monotonic drained triaxial tests were used.

In addition to the analyses using conventional strength parameters, a supplementary analysis was performed using the results of cyclic triaxial tests instead. In such analysis, two stages were considered: static analysis prior to the application of the seismic load, and dynamic analysis using pseudo-static approach. In the static analysis, the strength parameters (cohesion c and frictional angle ϕ) obtained from conventional tests were used. Since the calculated factor of safety, F_s, indicates the ratio of the shear resistance, τ_{sf}, and shear stress, τ_s, along the slip surface (i.e., $F_s = \tau_{sf} / \tau_s$), it is possible to estimate the average static shear stress along the slip plane from the known values of F_s and τ_{sf}. From Figure 11, the cyclic shear resistance ratios corresponding to N=20 cycles were read from the curves, and the data were used to plot the dynamic strength ratio, τ_d/τ_{sf}, as a function of the initial shear stress ratio, τ_s/τ_{sf}, as illustrated in Figure 14. Thus, knowing the average static shear stress along a slip plane, the corresponding cyclic resistance (or dynamic strength) can be estimated. The cyclic resistance is added to the initial static shear stresses and then used as strength parameters in performing the pseudo-static analysis to compute the F_s for the specified earthquake load. Note that in this procedure, it is tacitly assumed that the earthquake loading is applied for N=20 cycles.

In all the pseudo-static analysis conducted, the yield acceleration, k_y, corresponding to the limit equilibrium condition F_s=1.0 was calculated. For simplicity, the value of k_y was assumed to be constant throughout the duration of earthquake loading.

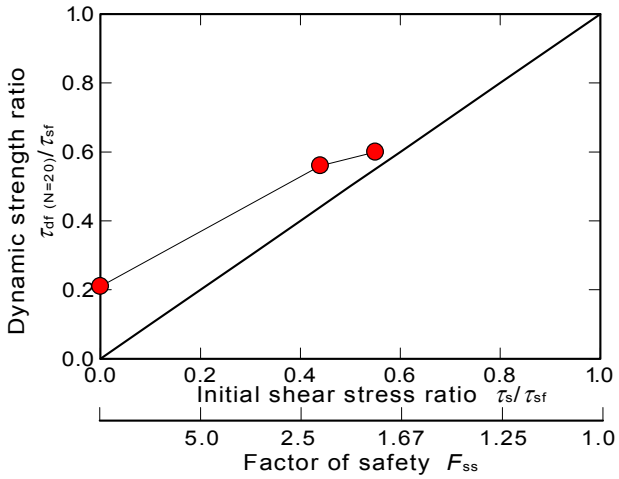

Figure 14. Relation between dynamic strength and initial stress obtained from triaxial test results

The results of the analyses are summarized in Table 3 for all the cases considered in terms of the yield acceleration, k_y, necessary for limit equilibrium condition (F_s=1.0). For cases with composite failure surfaces, the values for the two major slip surfaces considered are also indicated. Considering that the results of SHAKE analysis showed k_h values of 0.35-0.37, the only condition where k_y is less than these values is the case involving the use of dynamic strength at the slip surface; all other cases using conventional strength parameters resulted in higher value of k_y than that induced by the 2011 earthquake. For the conventional analysis to hold, k_h should at least be 0.39, or a PGA of 1,570 cm/sec^2; this value is too large.

Table 3. Results of pseudo-static analysis for the failed embankment in Block 1

Case	Condition	Strength Parameters	Yield acceleration, k_y	
			Slip 1	Slip 2
A	No water table; composite slip surfaces	c_d=9kN/m^3, ϕ=31.7^o	0.46	0.42
B-1	With water table; Composite slip surfaces		0.43	0.39
B-2	With water table: Cylindrical slip surface		0.42	
B-2’	With water table: Cylindrical slip surface	c_d=9kN/m^3, ϕ=31.7^o; then changed to dynamic strength	0.24	

Thus, based on the calculations presented above, it appears that the slope failure in Taiyo New Town can be attributed to the liquefaction of the fill, especially near the interface between the top fill layer and the highly weathered tuffaceous sandstone. With the development of excess pore water pressure, the fill underwent large deformation during the shaking induced by the gigantic Tohoku earthquake.

CONCLUSIONS

The gigantic 2011 off the Pacific coast of Tohoku Earthquake caused 5 slope failures in Taiyo New Town, a housing site on artificial valley fill in Yamamoto town, Miyagi Prefecture. To understand the mechanism of the slope failures, field inspection, strong motion record analyses, laboratory tests and slope stability analyses were conducted. The following are the major conclusions from this study:

1. The residential site of Taiyo New Town was constructed through cut and fill method. The original hilly ground consisted of weakly consolidated tuffaceous sandstone, which showed high degree of weathering towards the surface and manifested itself as sand on the surface. Thus, the fill material used to fill-up the valleys was generally sandy soil.
2. The maximum surface acceleration recorded in Yamamoto seismic station was 850-870 cm/sec^2 with predominant period of 4-6Hz. The estimated maximum acceleration on top of the fill based on seismic response analyses was 1170-1300 cm/sec^2.
3. Each of the five slope failures at the housing site was observed to occur at the boundary between the filled-up valley and the fill or on the shoulder of the embankment.
4. The sandy fill material has fines content *Fc*=20%. Even when compacted at 90% degree of compaction, the fill material showed very low internal friction angle and low liquefaction resistance. Moreover, the liquefaction resistance decreased with application of initial shear stress.
5. Pseudo-static slope stability analysis using conventional strength parameters cannot explain the slope failure in Block 1. However, when dynamic strength (or liquefaction resistance) was used to represent the soil strength at the slip surface, the yield seismic coefficient required to induce failure was lower than the estimated seismic coefficient on top of the fill.
6. The slope failure in Taiyo New Town can be attributed to the liquefaction of the fill material induced by the intense shaking. It was possible that during the earthquake, the ground water level was near the boundary of the original ground and the fill, making liquefaction possible.

ACKNOWLEDGMENTS

The authors would like to acknowledge the assistance of the engineering staff of Yamamoto Town Office for providing access to the site for inspection and for the valuable information during subsequent meetings. The strong motion data was obtained from K-Net.

REFERENCES

Geospatial Information Agency of Japan, GSI (2011). *Area Flooded by the Tsunami (Approximate)*, http://www.gsi.go.jp/common/000059734.pdf (in Japanese).

KiK-Net (2011). *Digital Strong Motion Network*, http://www.kik.bosai,go,jp/

Fukken Gijutsu Consultant Co. Ltd. (2008). *Ground Map of Built-up Residential Land*, 1:25,000 scale

Nakamura, Y., (1989). "A method for dynamic characteristics estimation of subsurface using microtremor on the ground surface," *Quarterly Report of Railway Technical Research Iinstitute*, Vol. 30, No. 1, 25 to 33.

Noda, S., Uwabe, T. and Chiba, T. (1975). "Relation between seismic coefficient and ground acceleration for gravity quay wall," *Report of the Port and Harbour Research Institute*, 14 (4) (in Japanese).

Hosono,Y. and Yoshimine, M. (2004). "Liquefaction of sand in simple shear condition," Proc., International Conference on Cyclic Behaviour of Soils and Liquefaction Phenomena, Bochum, Germany, 129-136.

Vaid, Y.P., Chung, E.K.F. and Kuerbis, R.H. (1990). "Stress path and steady state," Canadian Geotechnical Journal, 27(1): 1-7.

Hyodo, M., Murata, H., Yasufuku, N. and Fujii, T. (1991). "Undrained cyclic shear strength and residual strength of saturated sand by cyclic triaxial tests," *Soils and Foundations*, Vol. 31, No. 3, 60-76.

Hyodo, M., Tanimisu, H., Yasufuku, N. and Murata, H. (1994). "Undrained cyclic and monotonic behavior of saturated loose sand," *Soils and Foundations*, Vol. 34, No. 1, 19-32.

Japanese Geotechnical Society (2001). *Soil Testing Procedure and Commentary*, (in Japanese).